

## Synthesis of 2*H*-benzotriazole based donor-acceptor polymers bearing carbazole derivative as pendant groups: Optical, electronical and photovoltaic properties

I.A. Jessop<sup>1,\*</sup>, M. Bustos<sup>1</sup>, D. Hidalgo<sup>1</sup>, C.A. Terraza<sup>2</sup>, A. Tundidor-Camba<sup>2</sup>, M.A. Pardo<sup>2</sup>, D. Fuentealba<sup>3</sup>, M. Hssein<sup>4</sup>, J.C. Bernede<sup>5</sup>

<sup>1</sup> Universidad de Tarapacá, Facultad de Ciencias, Departamento de Química, Laboratorio de Materiales Orgánicos y Poliméricos, Av. General Velásquez 1775, Arica, Chile.

<sup>2</sup> Pontificia Universidad Católica de Chile, Facultad de Química, Departamento de Química Orgánica, Laboratorio de Polímeros, Av. Vicuña Mackenna 4860, Macul, Santiago, Chile.

<sup>3</sup> Pontificia Universidad Católica de Chile, Facultad de Química, Departamento de Química Física, Laboratorio de Estructuras Biosupramoleculares, Av. Vicuña Mackenna 4860, Macul, Santiago, Chile.

<sup>4</sup> Institut des Matériaux Jean Rouxel (IMN), CNRS, UMR 6502, 2 rue de la Houssinière, BP 32229, 44322 Nantes cedex 3, France.

<sup>5</sup> Université de Nantes, MOLTECH-Anjou, CNRS, UMR 6200, 2 rue de la Houssinière, BP 92208, Nantes, F-44000 France.

\*E-mail: [iajessop@uta.cl](mailto:iajessop@uta.cl)

Received: 25 August 2016 / Accepted: 4 October 2016 / Published: 10 November 2016

---

Four 2*H*-benzotriazole based D-A polymers bearing carbazole derivative as pendant groups and fluorene or thiophene as donor units (**P1-P4**) were designed and synthesized. These polymers combine good thermal stability and excellent solubility in common organic solvents. Spectroscopic measurements carried out for **P1**, **P2** and **P3** indicate that polymer backbone induces effective the quenching of the 3,6-di(thiophen-2-yl)-9*H*-carbazole (**CT**) fluorescence, implying an intramolecular Förster Resonance Energy Transfer (FRET) process. Preliminary investigations on the photovoltaic multiheterojunction devices based on **P1-P4** showed power conversion efficiencies (PCEs) of up to 1.7 % for **P1** and **P2** and close to 2.0 % for **P3**. This means that the polymer/ $\pi$ -conjugated pendant units structure is a promising alternative to improve the performance of organic solar cells.

---

**Keywords:** Donor-acceptor copolymers; pendant group; FRET; Electrochemical measurements; Optical and Photovoltaic properties

### 1. INTRODUCTION

Over the last couple of decades, there has been great interest in the study of conducting polymers (CPs) due their potential applications in organic light emitting diodes (OLEDs),-organic solar

cells (OSCs), organic field effect transistors (OFETs) and organic sensors [1-7]. Each of these applications requires materials with a specific set of both physical and electrochemical features. For example, CPs aimed as p-type materials for organic solar cells should have relative low optical bandgap with broad absorption spectrum to absorb as much sunlight as possible [8].

One approach to achieve CPs with low bandgap is based on the incorporation of alternating electron donating and electron accepting moieties in the conjugated polymer backbone (D-A polymers), which gives rise to intramolecular charge transfer interactions (ICT) [9]. Benzazoles are one of the most popular electron deficient units used for the synthesis of low bandgap polymers. Among all of the derivatives, our group became interested in 2*H*-benzotriazole (2*H*-BTz) moiety, which is a heteroaromatic compound with a moderate electron-accepting feature because of their polarizable imine groups (C=N) [8,10-11]. Furthermore, the easy modification of N-H bond of 2*H*-BTz unit can allow tuning of its structural and electronic properties to achieve processable 2*H*-BTz-containing polymers.

Several studies have described the electroluminescent, electrochromic and photovoltaic properties of D-A CPs based on 2*H*-BTz moiety [12-19]. Among all of these studies, the work of Tanimoto *et al.* attracted our attention. They reported the synthesis of poly(2*H*-benzotriazole)s bearing carbazole (CBz) units linked with alkyl chains to the backbones [20]. The authors suggest that an energy transfer process occurs between CBz and the poly(2*H*-BTz), which explains its red-shifted absorption.

Förster Resonance Energy Transfer (FRET) is a non-radiative process from a fluorescent emitter to a lower energy acceptor via long-range dipole-dipole interactions. The strength of this interaction is strongly dependent on the overlap integral between donor and acceptor units [21-23]. Recent studies in dye-sensitized solar cells have used the FRET process to improve the performance of OSCs devices [23-25]. In fact, a derivative of CBz (3,6-di(thiophen-2-yl)-9*H*-carbazole) has been used as FRET pair of fullerene (C<sub>60</sub>), from which a polymer with improved optical and electronic properties was obtained [26].

Taking into account all these ideas, we decide to synthesize four 2*H*-BTz-based CPs using 4,7-dibromo-2*H*-benzo[*d*][1,2,3]triazole (**BTz**) and 4,7-bis(5-bromothiophen-2-yl)-2*H*-benzo[*d*][1,2,3]triazole (**BTzT**) as acceptor units, and a fluorene derivative (**F**) and thiophene (**T**) as donor units. The CBz derivative 3,6-di(thiophen-2-yl)-9*H*-carbazole (**CT**) was linked to the backbone of the D-A polymers by a hexyl alkyl chain attached to the N-atom of the acceptors, in order to study its effect on the optical, electrochemical and photovoltaic properties of these polymers. The synthesized polymers (**P1-P4**) were characterized by <sup>1</sup>H-NMR, SEC and thermogravimetric analysis, UV-vis and fluorescence spectroscopies and cyclic voltammetry. The photovoltaic multiheterojunction devices based on **P1-P4** exhibit power conversion efficiencies (PCEs) of up to 1.7 % for **P1** and **P2** and close to 2.0 % for **P3**. A comparative study between **P1**-based device and a control device obtained from **P1** without **CT** substituents (**P-01**) showed that FRET process is a promising strategy to improve efficiency of OSCs.

## 2. EXPERIMENTAL

### 2.1. Materials

All reagents and solvents were used without further purification. 4,7-dibromobenzo[*c*][1,2,5]thiadiazole, 1,6-dibromohexane, 3,6-dibromocarbazole, 2-thienylboronic acid, tetrakis(triphenylphosphine)palladium(0) (Pd[PPh<sub>3</sub>]<sub>4</sub>), 9,9-dihexylfluorene-2,7-diboronic acid bis(1,3-propanediol)ester, 2,5-thiophenediylbisboronic acid, tetrabutylammonium bromide (TBAB), *N*-bromosuccinimide (NBS) and anhydrous 1,2-dimethoxyethane (DME) were purchased from Sigma-Aldrich (Milwaukee, WI, USA). Other reagents and solvents were obtained from Merck Millipore (Darmstadt, Germany). 3,6-dibromobenzene-1,2-diamine (**1**) and 4,7-dibromo-1*H*-benzo[*d*][1,2,3]triazole (**2**) were prepared according to previously described methods [27-28]. All other compounds were synthesized following the procedures described herein.

### 2.2. Instrumentation

<sup>1</sup>H and <sup>13</sup>C NMR spectra were recorded from a Bruker AVANCE III HD 400 spectrometer. Chemical shifts were reported as  $\delta$  values (ppm) relative to an internal tetramethylsilane (TMS) standard. Number-average ( $\bar{M}_n$ ) and weight-average ( $\bar{M}_w$ ) molecular weights were determined by size exclusion chromatography (SEC) at 25 °C with a high-pressure liquid chromatography (HPLC) Knauer pump, three PLgel 5 $\mu$ Mixed-C columns and static light-scattering (EA-02 Dawn Eos Enhanced Optical System) detector, using tetrahydrofuran (THF) as eluent. The calibration curve was made with a series of monodisperse polystyrene standards. Thermogravimetric analysis (TGA) measurements were performed with a Mettler Toledo TGA/DSC 1 Star-e thermobalance at a heating rate of 10 °C/min under nitrogen flow. The temperature of degradation ( $T_d$ ) corresponds to a 5 % weight loss. UV-vis absorption spectra were carried out with a HP8453 spectrophotometer using 1 cm path length quartz cells. For solid state measurements, polymer solutions were cast on indium tin oxide (ITO) coated glass plates. Fluorescence spectra were recorded using a LS55 PerkinElmer fluorescence spectrometer. The samples were excited at the wavelength of maximum absorption of the polymers in solution. Cyclic voltammograms (CV) were taken with a CH instrument, electrochemical workstation potentiostat, at a scan rate of 50 mV/s using polymer-coated slides as working electrodes, Ag/AgCl (in tetramethylammonium chloride solution) as reference electrode and Pt coil as counter electrode in an anhydrous and argon-saturated solution of 0.1 M of tetrabutylammoniumhexafluorophosphate (Bu<sub>4</sub>NPF<sub>6</sub>) in acetonitrile. The Ag/AgCl working electrode response was adjusted to match with the potential of saturated calomel electrode (SCE) response at 20 °C [29]. In these conditions, the oxidation onset potential ( $E_{on}^{ox}$ ) of ferrocene was 0.40 V versus SCE.

The photovoltaic properties of polymers were assessed with a glass/ITO/MoO<sub>3</sub>:CuI/Polymer/C<sub>60</sub>/Alq<sub>3</sub>/Al multiheterojunction device, where a 2:1 combination of MoO<sub>3</sub>:CuI was used as a double-anode buffer layer (ABL) and tris-(8-hydroxyquinoline)aluminum (Alq<sub>3</sub>) was used as an exciton-blocking layer (EBL) [30-31]. Before thin-film deposition, the ITO-coated glass substrates were scrubbed with soap, rinsed with distilled water, dried, and placed in the

vacuum chamber ( $10^{-4}$  Pa). The  $\text{MoO}_3$ ,  $\text{CuI}$ , polymers,  $\text{C}_{60}$ ,  $\text{Alq}_3$  and aluminum layers were deposited sequentially onto the substrate by sublimation. The thin-film deposition rates and thicknesses were estimated *in situ* using a quartz monitor. Current density versus voltage curves ( $J$ - $V$  characteristics) were measured using 300 W Oriel Instruments Solar Simulator and xenon lamp with AM 1.5G filter, at  $100 \text{ mW/cm}^2$  light intensity adjusted with a reference cell ( $0.5 \text{ cm}^2$  CIGS solar cell, calibrated at NREL, USA). Measurements were performed in ambient atmosphere. All devices were illuminated through TCO electrodes. Topographic images of glass/ITO/ABL/polymer devices were recorded using a JEOL 7600F microscope.

### 2.3. Synthesis and characterization of precursors and new acceptor/CT monomers (Scheme 1)

**3,6-Di(thiophen-2-yl)-9H-carbazole (CT)**. A mixture composed by 3,6-dibromo-9H-carbazole (0.98 g, 3.00 mmol), 2-thienylboronic acid (1.15 g, 9.00 mmol) and  $\text{Pd}[\text{PPh}_3]_4$  (0.53 g, 0.46 mmol) was purged under a steady stream of  $\text{N}_2$  for 30 min at room temperature. Anhydrous DME (55 mL) and degassed 2 M  $\text{K}_2\text{CO}_3$  (16 mL, 32.0 mmol) were then added and the reaction mixture was heated at  $85^\circ\text{C}$  for 24 h under  $\text{N}_2$ . After cooling to room temperature, water was added and the reaction mixture was extracted with ethyl acetate (3 x 50 mL). The combined organic layers were dried over anhydrous  $\text{Na}_2\text{SO}_4$  and filtered. The solvent was removed *in vacuo* and the residue was purified by flash chromatography on silica gel (hexane/ $\text{CH}_2\text{Cl}_2$ , 1:1 vol/vol) to afford a pale-yellow solid (0.94 g, 95 %).  $^1\text{H}$  NMR ( $\text{CDCl}_3$ , 400 MHz):  $\delta$  (ppm) 10.40 (s, 1H), 8.30 (s, 2H), 7.65 (dd, 2H), 7.42 (dd, 2H), 7.33 (d, 2H), 7.23 (d, 2H), 7.08 (m, 2H).  $^{13}\text{C}$  NMR ( $\text{CDCl}_3$ , 100 MHz):  $\delta$  (ppm) 145.24, 139.65, 127.64, 125.31, 124.05, 123.18, 122.95, 121.57, 117.14, 111.08.

**4,7-Dibromo-2-(6-bromohexyl)-2H-benzo[d][1,2,3]triazole (3)**. A mixture of compound **2** (1.00 g, 3.61 mmol), which was obtained from 4,7-dibromobenzo[*c*][1,25]thiadiazole according with the procedure showed in scheme 1, and  $\text{K}_2\text{CO}_3$  (1.85 g, 10.83 mmol) in DMF (20 mL) was stirred for 30 min at room temperature. The mixture was cooled to  $0^\circ\text{C}$  and then 1,6-dibromohexane (2.64 g, 10.83 mmol) was slowly added. The resulting solution was stirred for 48 h at room temperature. The reaction mixture was poured into ice-water bath and the crude was extracted with ethyl acetate (3 x 50 mL). The combined organic layers were dried over anhydrous  $\text{Na}_2\text{SO}_4$  and filtered. The solvent was removed *in vacuo* and the residue was purified by flash chromatography on silica gel (hexane/ethyl acetate, 20:1 vol/vol) to afford a pale-yellow oil (0.89 g, 56 %).  $^1\text{H}$  NMR ( $\text{CDCl}_3$ , 400 MHz):  $\delta$  (ppm) 7.43 (s, 2H), 4.78 (t, 2H), 3.38 (t, 2H), 2.16 (m, 2H), 1.85 (m, 2H), 1.50 (m, 2H), 1.40 (m, 2H).  $^{13}\text{C}$  NMR ( $\text{CDCl}_3$ , 100 MHz):  $\delta$  (ppm) 143.84, 129.70, 110.09, 57.31, 33.59, 32.48, 30.03, 27.62, 25.78.

**9-(6-(4,7-Dibromo-2H-benzo[d][1,2,3]triazol-2-yl)hexyl)-3,6-di(thiophen-2-yl)-9H-carbazole (BTz(CT))**. A mixture composed by **3** (0.68 g, 1.55 mmol), **CT** (0.50 g, 1.50 mmol), TBAB (0.12 g, 0.38 mmol), 50 % w/v KOH solution (18 mL) and toluene (7.5 mL) was heated to reflux for 24 h. After cooling at room temperature, water was added and the reaction mixture was extracted with ethyl acetate (3 x 50 mL). The combined organic layers were dried over anhydrous  $\text{Na}_2\text{SO}_4$  and filtered. The solvent was removed *in vacuo* and the residue was purified by flash chromatography on silica gel (hexane/ethyl acetate, 8:1 vol/vol) to afford a yellow-green solid (0.88 g, 85 %).  $^1\text{H}$  NMR ( $\text{CDCl}_3$ , 400

MHz):  $\delta$  (ppm) 8.35 (s, 2H), 7.73 (d, 2H), 7.44 (s, 2H), 7.37 (d, 2H), 7.34 (d, 2H), 7.29 (d, 2H), 7.13 (m, 2H), 4.74 (t, 2H), 4.27 (t, 2H), 2.11 (m, 2H), 1.88 (m, 2H), 1.42 (m, 4H).  $^{13}\text{C}$  NMR ( $\text{CDCl}_3$ , 100 MHz):  $\delta$  (ppm) 145.69, 143.83, 140.44, 129.71, 128.12, 126.13, 124.76, 123.85, 123.33, 122.27, 118.13, 110.08, 109.21, 57.27, 43.11, 29.98, 28.92, 26.72, 26.42.

*2-(6-Bromohexyl)-4,7-di(thiophen-2-yl)-2H-benzo[d][1,2,3]triazole (4)*. A mixture of **3** (0.34 g, 0.78 mmol), 2-thienylboronic acid (0.29 g, 2.30 mmol) and  $\text{Pd}[\text{PPh}_3]_4$  (0.14 g, 0.12 mmol) were purged under a steady stream of  $\text{N}_2$  for 30 min at room temperature. Anhydrous DME (14 mL) and degassed 2 M  $\text{K}_2\text{CO}_3$  (4.2 mL, 8.4 mmol) were then added and the reaction mixture was heated to reflux for 24 h under  $\text{N}_2$ . After cooling at room temperature, water was added and the reaction mixture was extracted with chloroform (3 x 50 mL). The combined organic layers were dried over anhydrous  $\text{Na}_2\text{SO}_4$  and filtered. The solvent was removed *in vacuo* and the residue was purified by flash chromatography on silica gel (hexane/ $\text{CH}_2\text{Cl}_2$ , 3:1 vol/vol) to afford a yellow-green oil (0.28 g, 80 %).  $^1\text{H}$  NMR ( $\text{CDCl}_3$ , 400 MHz):  $\delta$  (ppm) 8.09 (d, 2H), 7.64 (s, 2H), 7.38 (d, 2H), 7.19 (t, 2H), 4.83 (t, 2H), 3.40 (t, 2H), 2.22 (m, 2H), 1.88 (m, 2H), 1.56 (m, 2H), 1.47 (m, 2H).  $^{13}\text{C}$  NMR ( $\text{CDCl}_3$ , 100 MHz):  $\delta$  (ppm) 142.26, 140.05, 128.23, 127.08, 125.73, 123.73, 122.97, 56.72, 33.77, 32.63, 29.94, 27.71, 25.90.

*2-(6-Bromohexyl)-4,7-bis(5-bromothiophen-2-yl)-2H-benzo[d][1,2,3]triazole (5)*. To a solution of **4** (0.25 g, 0.56 mmol) in DMF (9 mL) was slowly added NBS (0.25 g, 1.40 mmol) at room temperature. The reaction mixture was stirred for 5 h in the dark. Then, water was added and the reaction mixture was extracted with ethyl acetate (3 x 50 mL). The combined organic layers were dried over anhydrous  $\text{Na}_2\text{SO}_4$  and filtered. The solvent was removed *in vacuo* and the residue was purified by flash chromatography on silica gel (hexane/ $\text{CH}_2\text{Cl}_2$ , 2:1 vol/vol) to afford a bright-yellow solid (0.26 g, 77 %).  $^1\text{H}$  NMR ( $\text{CDCl}_3$ , 400 MHz):  $\delta$  (ppm) 7.81 (d, 2H), 7.53 (s, 2H), 7.15 (d, 2H), 4.83 (t, 2H), 3.42 (t, 2H), 2.21 (m, 2H), 1.88 (m, 2H), 1.56 (m, 2H), 1.46 (m, 2H).  $^{13}\text{C}$  NMR ( $\text{CDCl}_3$ , 100 MHz):  $\delta$  (ppm) 141.62, 141.12, 131.08, 127.19, 122.87, 122.32, 113.12, 56.72, 33.95, 32.53, 29.77, 27.52, 25.72.

*9-(6-(4,7-Bis(5-bromothiophen-2-yl)-2H-benzo[d][1,2,3]triazol-2-yl)hexyl)-3,6-di(thiophen-2-yl)-9H-carbazole (BTzT(CT))*. A mixture of **5** (0.22 g, 0.37 mmol), **CT** (0.12 g, 0.36 mmol), TBAB (0.03 g, 0.09 mmol), 50 % w/v KOH solution (4.5 mL) and toluene (2 mL) was heated to reflux for 24 h. After cooling at room temperature, water was added and the reaction mixture was extracted with ethyl acetate (3 x 50 mL). The combined organic layers were dried over anhydrous  $\text{Na}_2\text{SO}_4$  and filtered. The solvent was removed *in vacuo* and the residue was purified by flash chromatography on silica gel (hexane/ethyl acetate, 8:1 vol/vol) to afford a bright-orange solid (0.24 g, 78 %).  $^1\text{H}$  NMR ( $\text{CDCl}_3$ , 400 MHz):  $\delta$  (ppm) 8.28 (s, 2H), 7.70 (d, 2H), 7.64 (d, 2H), 7.44 (s, 2H), 7.30 (d, 2H), 7.26 (d, 2H), 7.23 (d, 2H), 7.07 (m, 4H), 4.72 (t, 2H), 4.21 (t, 2H), 2.10 (m, 2H), 1.85 (m, 2H), 1.40 (m, 4H).  $^{13}\text{C}$  NMR ( $\text{CDCl}_3$ , 100 MHz):  $\delta$  (ppm) 145.71, 141.87, 141.30, 140.48, 131.03, 128.15, 127.04, 126.15, 124.76, 123.87, 123.36, 123.10, 122.43, 122.28, 118.15, 113.39, 109.20, 56.85, 43.20, 29.88, 28.99, 26.75, 26.53.

#### 2.4. Synthesis and characterization of D-A polymers (Scheme 2)

*Poly[BTz(CT)-alt-F] (P1)*. A mixture composed by **BTz(CT)** (0.35 g, 0.50 mmol), 9,9-dihexylfluorene-2,7-diboronic acid bis(1,3-propanediol)ester **F** (0.25 g, 0.50 mmol) and Pd[PPh<sub>3</sub>]<sub>4</sub> (0.03 g, 0.03 mmol) was purged under a steady stream of N<sub>2</sub> for 30 min at room temperature. Degassed toluene (10 mL) and 2 M K<sub>2</sub>CO<sub>3</sub> (2 mL, 4 mmol) were then added and the reaction mixture was heated to reflux for 72 h under N<sub>2</sub>. After cooling at room temperature, the reaction mixture was poured into methanol (100 mL) and the resulting solid was filtered through a Soxhlet thimble. The solid was extracted with acetone, hexane and finally with chloroform until the wash solution of each extraction was colorless. The solvent was removed from chloroform extract to afford a bright-green solid (0.38 g, 89 %). <sup>1</sup>H NMR (CDCl<sub>3</sub>, 400 MHz): δ (ppm) 8.34 (m, 2H), 8.20 (m, 2H), 8.10 (m, 2H), 7.91 (m, 2H), 7.81 (m, 2H), 7.71 (m, 2H), 7.34 (m, 4H), 7.24 (m, 2H), 7.09 (m, 2H), 4.86 (m, 2H), 4.28 (m, 2H), 2.25 (m, 4H), 2.11 (m, 2H), 1.95 (m, 2H), 1.54 (m, 4H), 1.13 (m, 12H), 0.92 (m, 4H), 0.77 (m, 6H).

*Poly[BTz(CT)-alt-T] (P2)*. This polymer was synthesized in accordance with the same procedure used for the preparation of **P1**. Thus, **BTz(CT)** (0.35 g, 0.50 mmol) and 2,5-thiophenediylbisboronic acid **T** (0.09 g, 0.50 mmol) were used as monomers to afford an orange solid (0.12 g, 38 %). <sup>1</sup>H NMR (CDCl<sub>3</sub>, 400 MHz): δ (ppm) 8.31 (m, 2H), 8.06 (m, 2H), 7.59 (m, 2H), 7.50 (m, 2H), 7.39 (m, 2H), 7.21 (m, 4H), 7.05 (m, 2H), 4.75 (m, 2H), 4.10 (m, 2H), 2.10 (m, 2H), 1.81 (m, 2H), 1.39 (m, 4H).

*Poly[BTzT(CT)-alt-F] (P3)*. **P3** was synthesized following the same procedure used for the preparation of **P1**. **BTzT(CT)** (0.32 g, 0.37 mmol) and **F** (0.19 g, 0.37 mmol) allowed to obtain bright-red solid (0.36 g, 94 %). <sup>1</sup>H NMR (CDCl<sub>3</sub>, 400 MHz): δ (ppm) 8.32(m, 2H), 8.13 (m, 2H), 7.67 (m, 10H), 7.46 (m, 2H), 7.31 (m, 4H), 7.24 (m, 2H), 7.08 (m, 2H), 4.84 (m, 2H), 4.23 (m, 2H), 2.18 (m, 2H), 2.06 (m, 4H), 1.86 (m, 4H), 1.61 (m, 2H), 1.25 (m, 2H), 1.07 (m, 14H), 0.76 (m, 6H).

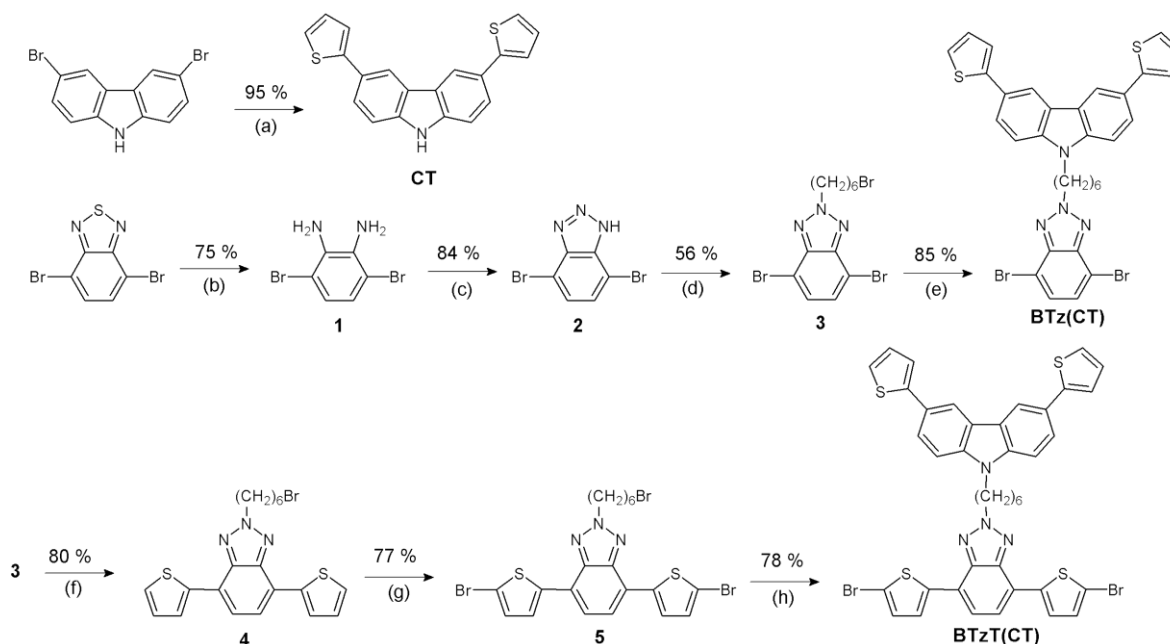
*Poly[BTzT(CT)-alt-T] (P4)*. From **BTzT(CT)** (0.22 g, 0.25 mmol) and **T** (0.04 g, 0.25 mmol) and following the same procedure used for the preparation of **P1**, it was possible to obtain **P4** as a violet solid (0.06 g, 32 %). <sup>1</sup>H NMR (CDCl<sub>3</sub>, 400 MHz): δ (ppm) 8.30 (m, 2H), 8.02 (m, 2H), 7.59 (m, 6H), 7.38 (m, 2H), 7.28 (m, 6H), 7.08 (m, 2H), 4.80 (m, 2H), 4.21 (m, 2H), 2.17 (m, 2H), 1.85 (m, 2H), 1.45 (m, 4H).

### 3. RESULTS AND DISCUSSION

#### 3.1. Synthesis and characterization of monomers and polymers

The synthetic routes of monomers are sketched in Scheme 1. Here it is possible to see that **BTz(CT)** and **BTzT(CT)** were synthesized in four and six steps; respectively, obtaining a general structure that contain acceptor, π-linker and π-conjugated moieties. Briefly, starting from 4,7-dibromobenzo[*c*][1,2,5]thiadiazole, a reduction reaction using a hydride derivative was performed to obtain 3,6-dibromobenzene-1,2-diamine (**1**) with a yield of 75 %. This aromatic diamine was used to synthesize 4,7-dibromo-1*H*-benzo[*d*][1,2,3]triazole (**2**) by a diazotization reaction, in a satisfactory

yield (84 %). This step was then followed by an alkylation reaction with 1,6-dibromohexane to get 4,7-dibromo-2-(6-bromohexyl)-2*H*-benzo[*d*][1,2,3]triazole (**3**) in 56 % yield. In this reaction,  $K_2CO_3$  was used as base and *N,N*-dimethylformamide (DMF) as solvent instead of the *t*-BuOK/ $CH_3OH$  system previously reported [18-19,32-33]. The 2*H* isomer was easily separated from 1*H* isomer by column chromatography. Once purified the dibromine derivative **3**, it was alkylated with 3,6-di(thiophen-2-yl)-9*H*-carbazole (**CT**) in transfer phase conditions to obtain monomer **BTz(CT)** in 85 % yield. For this, **CT** was prepared from a commercial precursor via Suzuki-Miyaura cross-coupling reaction with 2-thienylboronic acid (95 % yield), based on the methodology described by Nakamura *et al.* with slight modifications [34]. Compound **3** was also precursor of 2-(6-bromohexyl)-4,7-di(thiophen-2-yl)-2*H*-benzo[*d*][1,2,3]triazole (**4**, 80% yield), synthesized under the same reaction conditions used to prepare **CT**. The dibromination of **4** using NBS as the bromating agent allowed to obtain 2-(6-bromohexyl)-4,7-bis(5-bromothiophen-2-yl)-2*H*-benzo[*d*][1,2,3]triazole (**5**) with 77 % yield. Finally, **BTzT(CT)** was obtained from **5** in 78 % yield by alkylation reaction with **CT**, according to the same synthetic procedure used to prepare **BTz(CT)**.



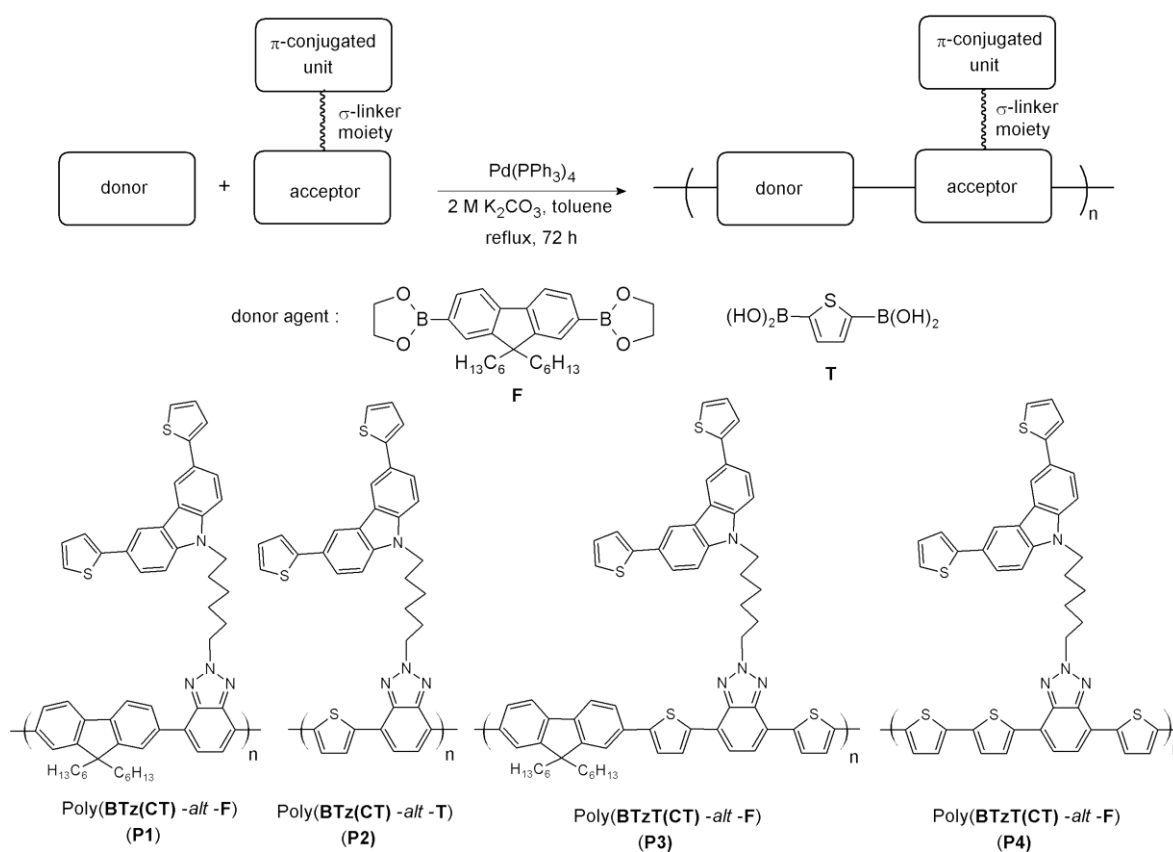
Reagents and conditions: (a) 2-thienylboronic acid,  $Pd[PPh_3]_4$ , 2 M  $K_2CO_3$ , DME, 85 °C, 24 h. (b)  $NaBH_4$ , ethanol, rt, 20 h. (c) acetic acid, 0 °C, 0.7 M  $NaNO_2$ , rt, 30 min. (d)  $K_2CO_3$ , DMF, 30 min, 0 °C, 1,6-dibromohexane, rt, 48 h. (e) **CT**, KOH 50 % w/v, TBAB, toluene, 100 °C, 24 h. (f) 2-thienylboronic acid,  $Pd[PPh_3]_4$ , 2 M  $K_2CO_3$ , DME, 85 °C, 24 h. (g) NBS, DMF, rt, 5 h. (h) **CT**, KOH 50 % w/v, TBAB, toluene, 100 °C, 24 h.

**Scheme 1.** Synthetic route of the new acceptor/CT monomers; **BTz(CT)** and **BTzT(CT)**.

The scheme 2 shows the repetitive unit of each polymer and also a schematization of the preparation route pointing out the donor and acceptor nature of the monomers. D-A polymers (**P1-P4**) were synthesized by Suzuki polycondensation reactions using equivalent amounts of the acceptor/CT monomers, **BTz(CT)** and **BTzT(CT)**, and the donor monomers, **F** and **T**. The polymers were purified

by continuous extractions with acetone, hexane and finally with chloroform. The chloroform soluble fractions were isolated to afford poly[BTz(CT)-alt-F] (**P1**), poly[BTz(CT)-alt-T] (**P2**), poly[BTzT(CT)-alt-F] (**P3**) and poly[BTzT(CT)-alt-T] (**P4**) with 89 %, 38 %, 94 % and 32 % yields; respectively. Because of the alkyl chains attached to the fluorene units improve the solubility of the polymer chains as they grow during the polymerization reaction, **P1** and **P3** shows higher yields than those based on thiophene monomer (**P2** and **P4**).

After purification, size-exclusion chromatography (SEC) experiments, based on monodisperse polystyrene standards and using tetrahydrofuran (THF) as eluent were carried out. Number-average molecular weight ( $\bar{M}_n$ ) and polydispersity indexes (PDI) for each polymer are shown in table 1.



**Scheme 2.** Schematic representation of the synthetic route for polymers and their repetitive units.

### 3.2. Thermal properties

Thermogravimetric analysis (TGA) was carried out to evaluate the thermal stability of the polymers. As can be seen in Figure 1 and Table 1, the four polymers presents good thermal stability with less than 5 % weight loss ( $T_d$ ) at temperatures up to 400 °C, which is high enough for their application in OSCs. These values are in the same range to those obtained for polymers with very similar backbone than P1 and P3 but without CT pendant unit, previously published [13-14, 17]. Moreover, such quite high thermal stability allows depositing the polymer in vacuum maintaining the sublimation crucible at a temperature below 400 °C.

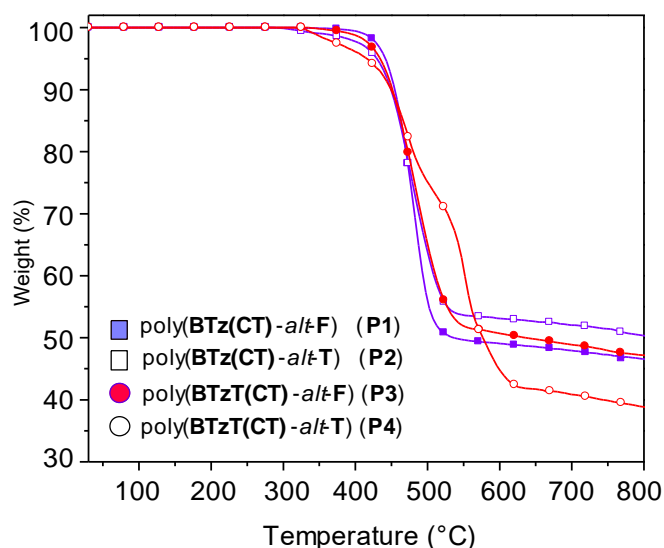


**Figure 1.** TGA thermograms of polymers **P1-P4**.

### 3.3. Optical properties

The UV-vis absorption spectra of polymers in dilute solutions of chloroform ( $10^{-6}$  M) and in thin films are shown in Figure 2. The absorption bands between 350 and 580 nm (Table 1) are attributed mainly to the intra-molecular charge transfer (ICT) between the electron-donor and electron-acceptor units [7,9,35]. Because of the aggregation and stronger intermolecular  $\pi$ - $\pi$  interactions between the conjugated main chains of polymers in solid state, all the absorption peaks are red-shifted from solution to film.

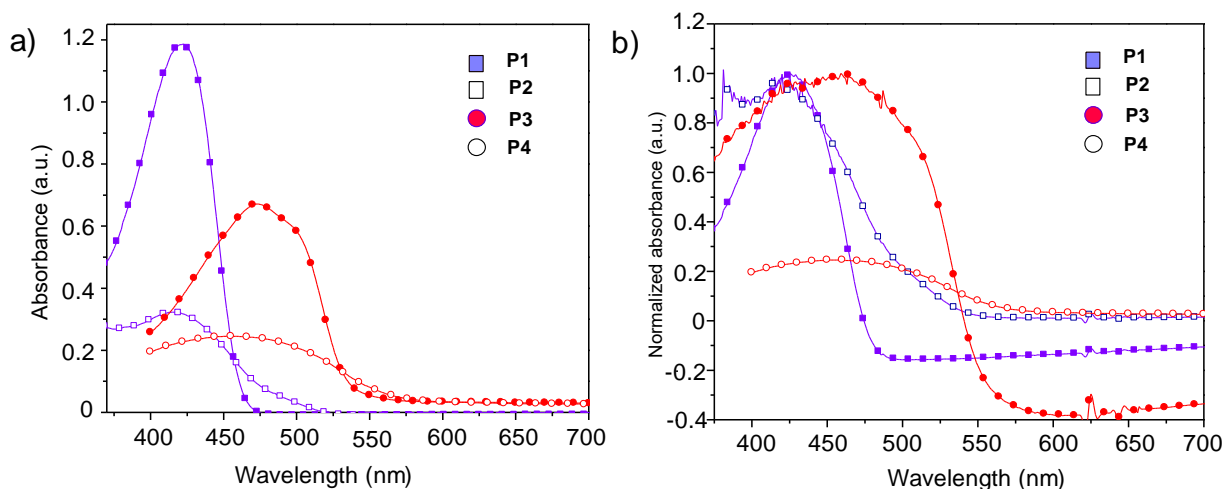


**Figure 2.** UV-vis spectra of polymers (a) in dilute solutions of  $\text{CHCl}_3$  and (b) in solid state.

The absorption spectra of **P1**, **P2**, **P3** and **P4** films have absorption edges at 478, 539, 553 and 563 nm, corresponding to optical bandgaps ( $E_g^{opt}$ ) of 2.59, 2.30, 2.24 and 2.20 eV, respectively. It

should be noted that these  $E_g^{opt}$  values are slightly higher than those reported in literature. The absorption bands of the polymers in solid state are blue-shifted compared to the absorption bands of the polymers with similar structure but without **CT** unit [13-17]. However, the trend in the series is the same, **P1** have the widest  $E_g^{opt}$  and **P4** have the narrowest  $E_g^{opt}$ .

As can be seen, the  $E_g^{opt}$  of polymers based on **BTzT(CT)** as acceptor and thiophene as donor are lower than those based on **BTz(CT)** as acceptor and fluorene as donor. Apparently, the addition of thiophene spacers between the electron-poor benzotriazole moiety and its use as donor units increases the conjugation in the main chain, which decreases the bandgap values.

Additionally, the UV-vis absorption spectrum of a solution of **CT** at the same molar concentration was also obtained. The spectrum shows an absorption band centered at 315 nm with no significant absorbance beyond 390 nm, which implies a limited overlapping with absorption bands of the polymers. This fact ensures that the light absorption of the polymers will not be inhibited by the **CT** pendant unit.

Figure 3 shows the fluorescence spectra of **P1-P4** and **CT** in chloroform solutions ( $10^{-6}$  M). The maximum fluorescence peaks of the polymers are observed between 465 and 590 nm approximately (Table 1). On the other hand, the **CT** unit shows an emission peak at 402 nm, which strongly overlaps with the absorption bands of **P1**, **P2** and **P3**, making promissory FRET pairs. As can be seen in Figure 4, when a solution of **P1** is excited at 315 nm, the wavelength of maximum absorption of **CT**, the only peak observed is centered at 469 nm. Therefore, the fluorescence of **CT** is quenched by **P1**. This fact is generally considered as an evidence of the FRET process [36-40].

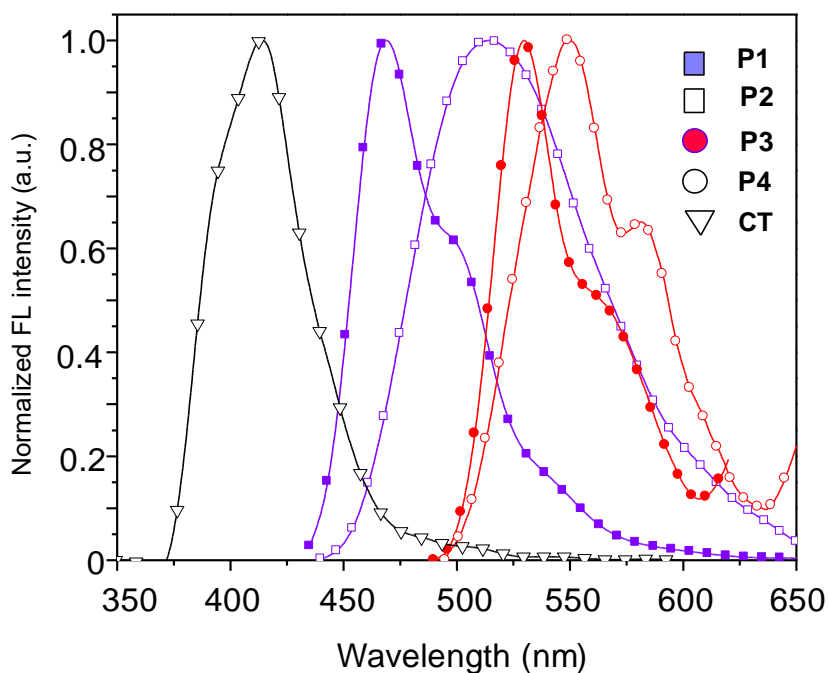


**Figure 3.** Normalized fluorescence spectra of polymers and **CT** unit in dilute solution of  $\text{CHCl}_3$ .

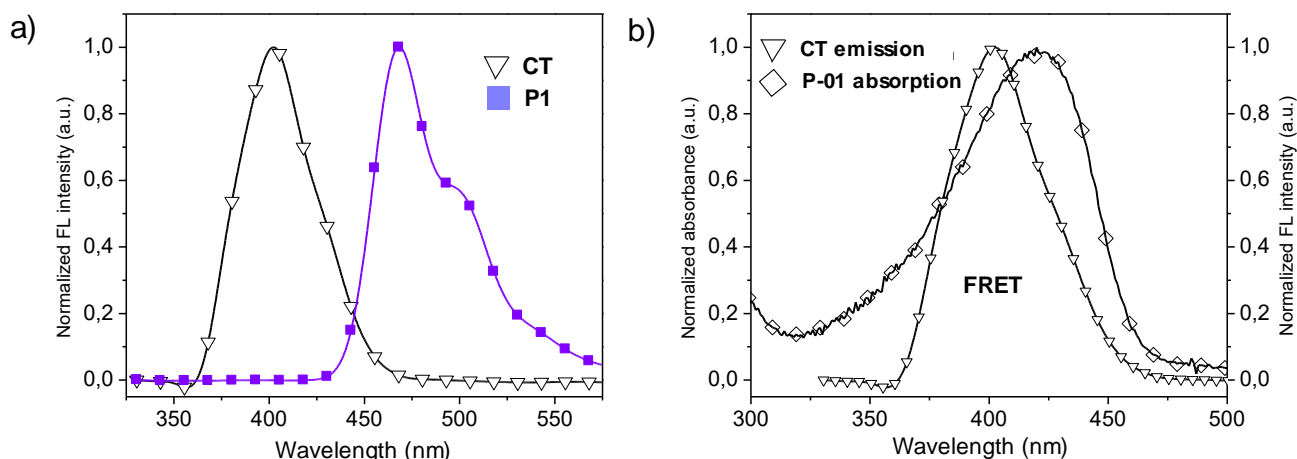


**Figure 4.** a) Normalized fluorescence spectra of **P1** and **CT** solutions at 315 nm excitation wavelength, confirming occurrence of FRET process. b) Normalized absorption spectrum of **P1** without **CT** pendant unit (**P-01**) and normalized fluorescence spectrum of **CT**.

### 3.4. Electrochemical properties

Cyclic voltammetry (CV) measurements were carried out using working electrodes prepared by immersing ITO slides into  $\text{CHCl}_3$  solutions of each polymer (10 mg/mL). The potential window used was between -2.0 and +2.0 V versus Ag wire pseudo-reference electrode for all experiments. As shown in Figure 5, all polymers present an oxidation or anodic process and a cathodic process or reduction. Furthermore, the HOMO and LUMO energy levels of **P1-P4** were calculated from the oxidation onset potentials ( $E_{on}^{ox}$  vs SCE) and the reduction onset potentials ( $E_{on}^{red}$  vs SCE); respectively, assuming SCE electrode to be -4.8 eV from vacuum [41-44]. These results are summarized in Table 1 along with the electrochemical bandgaps ( $E_g^{elec}$ ). The differences between  $E_g^{opt}$  and  $E_g^{elec}$  are within experimental error (0.2-0.5 eV) [19].

As seen in table 1, **P2** presents higher HOMO level than **P1**. This could be attributed to the replacement of fluorene for electron-rich thiophene as donor moiety. Because of LUMO level mainly depends on the acceptor unit, no significant differences between the LUMOs of **P1** and **P2** are observed. The same trends are observed between **P4** and **P3**. On the other hand, when the acceptor unit **BTz(CT)** is replaced by **BTzT(CT)**, the HOMO and LUMO levels tend to increase. It should be noted that the HOMO energies of **P1-P4** match very well with those previously reported for the same polymers without the carbazole derivative unit [14-16]. Nevertheless, slightly differences between the LUMOs of **P1** and **P3** with literature are detected.

Interestingly, the voltammogram of **P1** shows a little peak centered at about 0.3 V (Figure 5). According to Sadki *et al.*, this signal corresponds to the onset of the oxidative polymerization of **CT** derivative [26]. However, this peak is observed at the same potential during subsequent cycles, which means that could be attributed to an oxidative-type doping of the **CT** moiety.

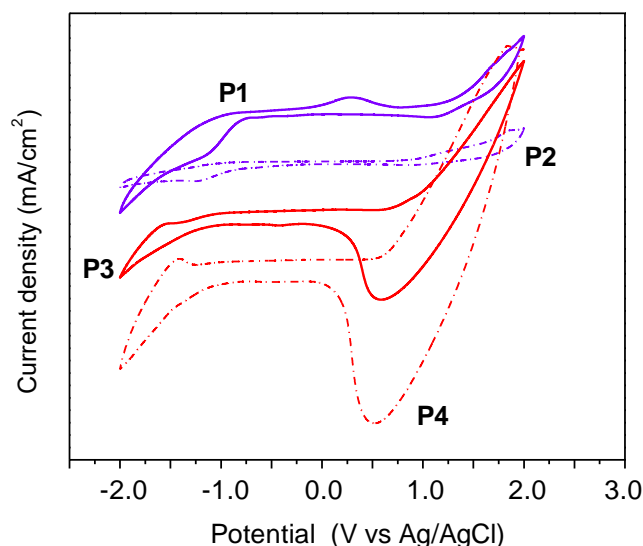


**Figure 5.** Cyclic voltammograms (second scan) of polymer films cast on ITO-coated glass.

**Table 1.** Physical properties of D-A polymers

	$\bar{M}_n$ (kg/mol) <sup>a</sup>	PDI <sup>a</sup>	$T_d$ (°C) <sup>b</sup>	$\lambda_{\max}^{\text{sol}}$ (nm) <sup>c</sup>	$\lambda_{\max}^{\text{film}}$ (nm) <sup>d</sup>	$\lambda_{\max}^{\text{em}}$ (nm) <sup>e</sup>	$E_{\text{HOMO}}$ (eV) <sup>f</sup>	$E_{\text{LUMO}}$ (eV) <sup>g</sup>	$E_g^{\text{elec}}$ (eV) <sup>h</sup>
<b>P1</b>	49	3.64	441	422	425	469/501	-5.64	-3.58	2.06
<b>P2</b>	3	1.34	430	415	425	514	-5.28	-3.54	1.74
<b>P3</b>	7	1.95	434	463	467	530/567	-5.21	-3.23	1.98
<b>P4</b>	20	1.07	416	455	460	549/582	-5.02	-3.15	1.87

<sup>a</sup> Number-average molecular weight and polydispersity index determined by SEC, respectively. <sup>b</sup> Temperature at 5 % weight loss. <sup>c</sup> Absorption maximum taken from UV-vis spectra of polymer in dilute solution of  $\text{CHCl}_3$ . <sup>d</sup> Absorption maximum taken from UV-vis spectra of polymer in solid state. <sup>e</sup> Emission maximum and vibronic shoulder taken from fluorescence spectra. <sup>f</sup>  $E_{\text{HOMO}} = -e(E_{\text{on}}^{\text{ox}} + 4.4)$  eV. <sup>g</sup>  $E_{\text{LUMO}} = -e(E_{\text{on}}^{\text{red}} + 4.4)$  eV. <sup>h</sup>  $E_g^{\text{elec}} = -e(E_{\text{HOMO}} - E_{\text{LUMO}})$  eV.

### 3.5. Photovoltaic properties

Organic solar cells were fabricated with a device structure of glass/ITO/MoO<sub>3</sub>:CuI/polymer/C<sub>60</sub>/Alq<sub>3</sub>/Al, where synthesized polymers were used as the electron donors and C<sub>60</sub> was used as the electron acceptor. Each device was optimized by studying the thickness of the different layers to achieve balanced and high values of  $V_{\text{oc}}$ ,  $J_{\text{sc}}$ ,  $FF$  and PCE. Besides, it should be noted that at least six diodes are realized by cycle of deposit to average the OSC performance values. In order to investigate the influence of the pendant CT moiety on the polymer backbone as well as elucidate its photophysical interaction, a reference-compound (**P-01**, Figure 6) was also prepared and analyzed. The backbone of **P-01** is the same that shows **P1** but without CT substituent and presents the following parameters:  $\bar{M}_n = 30$  kg/mol, PDI = 2.17 and  $E_g^{\text{opt}} = 2.47$  eV. The current-

voltage ( $J/V$ ) characteristics of **P1-P4**, including **P-01**, are shown in Figure 6 and the results are summarized in Table 2.

As seen in Table 2, **P1**, **P2** and **P3** showed overall PCEs of up to 1.7 %. Specifically, the best photovoltaic performance was obtained for **P3**; polymer based on fluorene as electron-donor unit and **BTzT(CT)** as electron-acceptor moiety. Both the planarity of fluorene unit and the incorporation of thiophenes moieties between benzotriazole would increase the conjugation along polymer backbone and would reduce its optical bandgap, which would allow harvest more photons from sunlight.

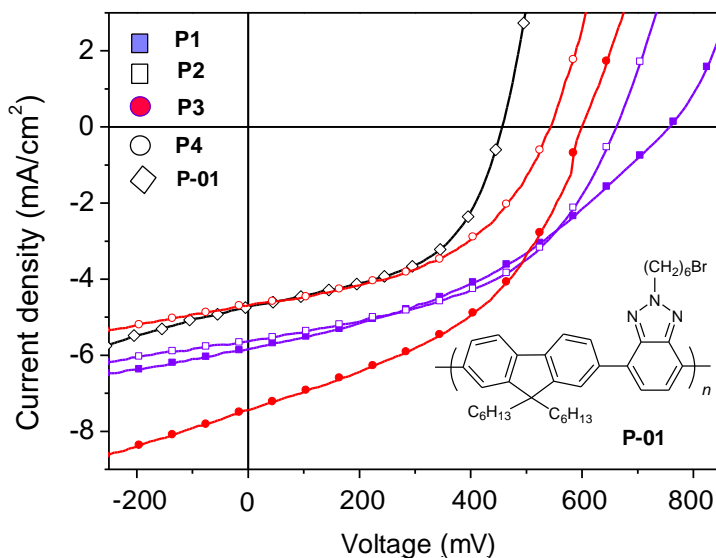


**Figure 6.**  $J$ - $V$  curves of the photovoltaic devices based on **P1-P4** and the reference polymer (**P-01**) under  $100 \text{ mW/cm}^2$  AM 1.5 G irradiation.

Deep-lying HOMO levels mean a higher open circuit voltage ( $V_{oc}$ ) which can be expected from OSCs because  $V_{oc}$  is linearly correlated with the difference of the HOMO of the donor and the LUMO of the acceptor [19]. The  $V_{oc}$  values of the devices fabricated from benzotriazole-based polymers range between 0.54 and 0.75 (Table 2). Theoretical  $V_{oc}$  can be calculated using a semi-empirical estimation equation [45], based on electrochemical data and considering a LUMO level for  $C_{60}$  at  $-4.5 \text{ eV}$ . Thus, the calculated  $V_{oc}$  for **P1**, **P2**, **P3** and **P4** are 0.84 V, 0.48 V, 0.41 V and 0.22 eV, respectively. Because of the difficulty of measuring precisely the energy level of frontier orbitals by solid-state cyclic voltammetry [46], these results are different from those shown in Table 2. However, the trend between these two  $V_{oc}$  series is the same, with an order **P1** > **P2** > **P3** > **P4**. In this sense, we believe that higher  $V_{oc}$  values and better efficiencies could be obtained by using an acceptor material with higher electron affinity than  $C_{60}$ , like  $C_{70}$  or  $PC_{70}BM$ .

The incorporation of **CT** units along the **P1** backbone led to significant enhancement in the  $V_{oc}$  and  $J_{sc}$  values compared to the control device. Indeed, the poor FRET process occurring between **P4** and **CT** could explain the lower performance of the **P4**-based device. These results demonstrate that FRET process is a promising strategy to improve efficiency of OSCs.

**Table 2.** Photovoltaic parameters and efficiencies of multiheterojunction solar cells devices.

	Thickness (nm)	$V_{oc}^a$ (V)	$J_{sc}^b$ (mA/cm <sup>2</sup> )	$FF^c$ (%)	PCE <sup>d</sup> (%)
<b>P1</b>	16	0.75	5.84	40	1.75
<b>P2</b>	16	0.68	5.63	48	1.78
<b>P3</b>	16	0.60	7.64	44	1.96
<b>P4</b>	18	0.54	4.69	48	1.20
<b>P-01</b>	5	0.46	4.72	52	1.11

<sup>a</sup> Open circuit voltage. <sup>b</sup> Short current density. <sup>c</sup> Fill factor. <sup>d</sup> Power conversion efficiency.

### 3.6. SEM analysis

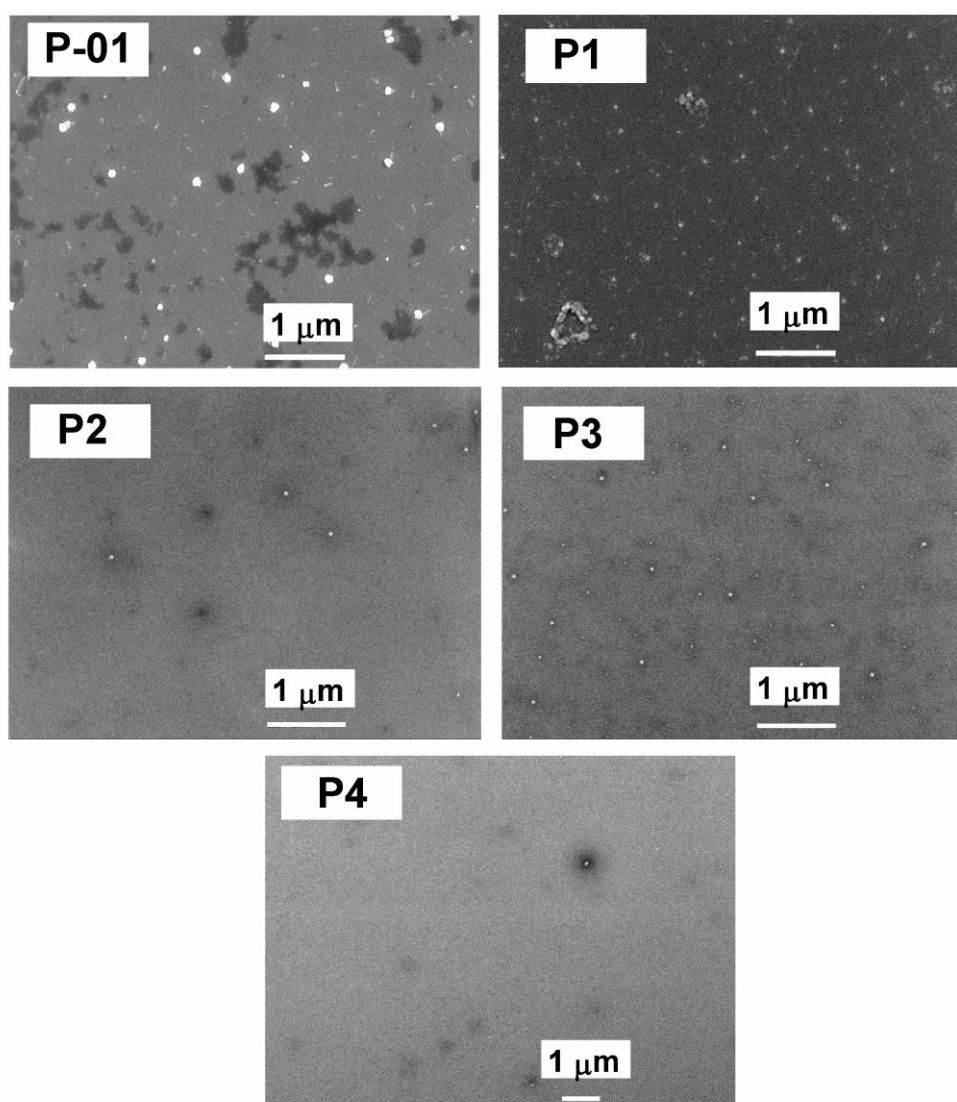


**Figure 7.** SEM images of polymers deposited on glass/ITO/MoO<sub>3</sub>:CuI substrates.

Interfacial morphology plays a crucial role in both charge collection and transport in OSCs devices. Greater surface roughness over the electrode surface can cause formation of defects which can

decrease the device efficiency [47]. SEM studies were carried out to investigate the film morphology of polymers deposited on glass/ITO/MoO<sub>3</sub>:CuI substrates. As can be seen in Figure 7, less homogeneous surface is observed for the **P-01** deposit compared to the **P1** deposit, which would also explain the better photovoltaic performance of the **P1** based device.

SEM images show relatively smooth surfaces for **P2**, **P3** and **P4** deposits. From this result, it is clear that the  $\pi$ - $\pi$  stacking interactions between polymer backbone and **CT** pendant units cause more ordered agglomerates. The homogeneous topography of the **P3** deposit, together with the high value of  $J_{sc}$  shown by the corresponding device, leads to the best PCE close to 2.0 %. These results indicate the potential for improving OSCs performance via the functionalization of D-A polymers with  $\pi$ -conjugated units appropriately chosen to make good FRET pairs.

#### 4. CONCLUSIONS

Four alternating and thermally stable D-A copolymers based on 2*H*-benzotriazole derivatives as acceptor units and fluorene or thiophene as donor agents were synthesized (**P1-P4**). Their structural characterization was developed by NMR and SEC solution techniques. Thus, 3,6-di(thiophen-2-yl)-9*H*-carbazole **CT** was used as pendant unit in order to study its effect on the optical, electrochemical and photovoltaic properties of the polymers. Quenching of **CT** fluorescence was observed in chloroform diluted solutions of **P1-P3**, indicating that an intramolecular energy transfer takes place between the carbazole derivative and the polymer backbone. The copolymers present optical bandgaps ranging from 2.59 to 2.20 eV, HOMO energy levels between -5.64 and -5.02 eV and LUMO energy levels between -3.58 to -3.15 eV. Photovoltaic multiheterojunction devices were fabricated with glass/ITO/MoO<sub>3</sub>:CuI/polymers/C<sub>60</sub>/Alq<sub>3</sub>/Al architecture. A PCE close to 2.0 % was obtained for **P3** (fluorene as donor unit and dithienylbenzotriazole/**CT** as acceptor unit. The smooth surface of its deposit, due the  $\pi$ - $\pi$  stacking interactions between polymer backbone and **CT** moiety, and its high  $J_{sc}$  value would explain this promisingly high PCE. A comparative study on devices based on **P1** and a reference compound (a polymer with the same backbone as that of **P1** but without **CT** units) proves that FRET process between correctly chosen  $\pi$ -conjugated pendant units and polymer backbone is a promising strategy to obtain organic solar cells with better photovoltaic performances.

#### ACKNOWLEDGEMENTS

The authors would like to thank Dr. A. Leiva and Dr. M. A. del Valle from Pontificia Universidad Católica de Chile and Dr. C. Castro from Universidad de Tarapacá for their valuable assistance. This work was supported by the Comisión Nacional de Investigación Científica y Tecnológica, CONICYT, through project FONDECYT POSTDOCTORADO N° 3140609.

#### References

1. I. Botiz, S. Astilean, N. Stingelin, *Polym. Int.*, 65 (2016) 157.
2. S. Ho, S. Liu, Y. Chen, F. So, *J. Photon. Energy*, 5 (2015) 057611.
3. L. Lu, T. Zheng, Q. Wu, A. M. Schneider, D. Zhao, L. Yu, *Chem. Rev.*, 115 (2015) 12666.

4. J. You, L. Dou, Z. Hong, G. Li, Y. Yang, *Prog. Polym. Sci.*, 38 (2013) 1909.
5. H. Siringhaus, *Adv. Mater.*, 26 (2014) 1319.
6. Y. H. Chou, H. C. Chang, C. L. Liu, W. C. Chen, *Polym. Chem.*, 6 (2015) 341.
7. R. P. Singh, *Int. J. Electrochem.*, 7 (2012) 502707.
8. A. Pron, M. Leclerc, *Prog. Polym. Sci.*, 38 (2013) 1815.
9. L. Bian, E. Zhu, J. Tang, W. Tang, F. Zhang, *Prog. Polym. Sci.*, 37 (2012) 1292.
10. D. G. Patel, F. Feng, Y. Y. Ohnishi, K. A. Abboud, S. Hirata, K. S. Schanze, J. R. Reynolds, *J. Am. Chem. Soc.*, 134 (2012) 2599.
11. A. Balan, D. Baran, L. Toppare, *Polym. Chem.*, 2 (2011) 1029.
12. J. L. Banal, J. Subbiah, H. Graham, J. K. Lee, K. P. Ghiggino, W. W. H. Wong, *Polym. Chem.*, 4 (2013) 1077.
13. B. Liu, S. Ye, Y. Zou, B. Peng, Y. He, K. Zhou, *Macromol. Chem. Phys.*, 212 (2011) 1489.
14. E. Kaya, A. Balan, D. Baran, A. Cirpan, L. Toppare, *Org. Electron.*, 12 (2011) 202.
15. A. Balan, D. Balan, L. Toppare, *J. Mater. Chem.*, 20 (2010) 9861.
16. G. Hizalan, A. Balan, D. Baran, L. Toppare, *J. Mater. Chem.*, 21 (2011) 1804.
17. E. Kaya, D. H. Apaydin, D. E. Yildiz, L. Toppare, A. Cirpan, *Sol. Energ. Mat. Sol. Cells*, 99 (2012) 321.
18. V. Murugesan, R. Bettignies, R. Mercier, S. Guillerez, L. Perrin, *Synth. Met.*, 162 (2012) 1037.
19. B. Peng, A. Najari, B. Liu, P. Berrouard, D. Gendron, Y. He, K. Zhou, M. Leclerc, Y. Zou, *Macromol. Chem. Phys.*, 211 (2010) 2026.
20. A. Tanimoto, T. Yamamoto, *Macromolecules*, 39 (2006) 3546.
21. J. R. Lakowicz, *Principles of Fluorescence Spectroscopy*, Springer, (2006) New York, USA.
22. A. R. Clapp, I. L. Medintz, J. M. Mauro, B. R. Fisher, M. G. Bawendi, H. Mattoussi, *J. Am. Chem. Soc.*, 126 (2004) 301.
23. J. S. Huang, T. Goh, X. Li, M. Y. Sfeir, E. A. Bielinski, S. Tomasulo, M. L. Lee, N. Hazari, A. D. Taylor, *Nat. Photon.* 7 (2013) 479.
24. M. Lanzi, L. Paganin, F. Errani, *Polymer*, 53 (2012) 2134.
25. C. L. Wang, W. B. Zhang, R. M. Van Horn, Y. Tu, X. Gong, S. Z. D. Cheng, Y. Sun, M. Tong, J. Seo, B. B. Y. Hsu, A. J. Heeger, *Adv. Mater.*, 23 (2011) 2951.
26. N. Berton, I. Fabre-Francke, D. Bourrat, F. Chandezon, S. Sadki, *J. Phys. Chem. B*, 113 (2009) 14087.
27. Y. Tsubata, T. Suzuki, T. Miyashi, *J. Org. Chem.*, 57 (1992) 6749.
28. C. R. Bridges, T. M. McCormick, G. L. Gibson, J. Hollinger, D. S. Seferos, *J. Am. Chem. Soc.*, 135 (2013) 13212.
29. G. A. East, M. A. del Valle, *J. Chem. Ed.*, 77 (2000) 97.
30. L. Cattin, J. C. Bernède, Y. Lare, S. Dabos-Seignon, N. Stephant, M. Morsli, P. P. Zamora, F. R. Díaz, M. A. del Valle, *Phys. Status Solidi A*, 210 (2013) 802.
31. J. C. Bernède, L. Cattin, M. Morsli, S. R. B. Kanth, S. Patil, N. Stephant, *Energy Procedia*, 31 (2012) 81.
32. A. Tanimoto, T. Yamamoto, *Adv. Synth. Catal.*, 346 (2004) 1818.
33. N. Akbaşoğlu, A. Balan, D. Balan, A. Cirpan, L. Toppare, *J. Polym. Sci., Part A: Polym. Chem.* 48 (2010) 5603.
34. S. I. Kato, S. Shimizu, H. Taguchi, A. Kobayashi, S. Tobita, Y. Nakamura, *J. Org. Chem.*, 77 (2012) 3222.
35. X. Guo, M. Baumgarten, K. Müllen, *Prog. Polym. Sci.*, 38 (2013) 1832.
36. K. Meng, Q. Ding, S. Wang, Q. Gong, *Chem. Phys. Lett.*, 515 (2011) 155-158.
37. A. L. Rogach, *Nano Today*, 6 (2011) 355-365.
38. H. Yan, D. Li, Y. Zhang, Y. Yang, Z. Wei, *J. Phys. Chem. C*, 118 (2014) 10552.
39. R. Gao, Y. Cui, X. Liu, L. Wang, *Sci. Rep.* 4 (2014) 5570.

40. A. Diac, M. Focsan, C. Socaci, A. M. Gabudean, C. Farcau, D. Maniu, E. Vasile, A. Terec, L. M. Veca, S. Astilean. *RSC Adv.* 5 (2015) 77662.
41. F. Liang, F. Shi, Y. Fu, L. Wang, X. Zhang, Z. Xie, Z. Su, *Sol. Energ. Mat. Sol. Cells*, 94 (2010) 1803.
42. J. Y. Lee, K. W. Song, J. R. Ku, T. H. Sung, D. K. Moon, *Sol. Energ. Mat. Sol. Cells*, 95 (2011) 3377.
43. L. Longo, C. Carbonera, A. Pellegrino, N. Perin, G. Schimperia, A. Tacca, R. Po, *Sol. Energ. Mat. Sol. Cells*, 97 (2012) 139.
44. J. H. Kim, H. U. Kim, D. Mi, S. H. Jin, W. S. Shin, S. C. Yoon, I. N. Kang, D. H. Hwang, *Macromolecules*, 45 (2012) 2367.
45. M. C. Scharber, D. Mühlbacher, M. Koppe, P. Denk, C. Waldauf, A. J. Heeger, C. J. Brabec, *Adv. Mater.*, 18 (2006) 789.
46. N. Allard, N. Zindy, P. O. Morin, M. M. Wienk, R. A. J. Janssen, M. Leclerc, *Polym. Chem.*, 6 (2015) 3956.
47. S. Das, T. L. Alford, *J. Appl. Phys.*, 116 (2014) 044905.

© 2016 The Authors. Published by ESG ([www.electrochemsci.org](http://www.electrochemsci.org)). This article is an open access article distributed under the terms and conditions of the Creative Commons Attribution license (<http://creativecommons.org/licenses/by/4.0/>).